

# CLASSICAL MOLECULAR DYNAMICS (MD) SIMULATION OF SALT AND SOLVENT SOLVATION EVENTS IN LITHIUM ION BATTERIES TO DETERMINE ENERGY FLUCTUATIONS

Hubertus Ngaderman\*, Ego Srivajawaty Sinaga , Benny Abraham Bungasalu

Department of Physics, Mathematic and Natural Science of Faculty, University of Cenderawasih  
Jl. Kamwolker perumnas 3 Jayapura 99333, Indonesia

{ Received: 24<sup>th</sup> September 2024; Revised: 13<sup>rd</sup> March 2025; Accepted: 10<sup>th</sup> April 2025 }

## ABSTRACT

This study looks at how salt and solvent mix, as shown by the final positions of particles in a simulation. The simulation uses Lennard-Jones parameters and runs in a closed system with fixed energy. The goal is to see if the particles follow the Maxwell velocity distribution. When lithium hexafluorophosphate salt mixes with ethylene carbonate, solvation occurs. The simulation runs for 100 and 2000 steps to get accurate results. At the start, no chemical reactions or outside forces are involved just the natural movement of particles. For fluorine, after 2000 steps, the particles start to group in one area, showing the system isn't balanced yet. Since velocity is linked to kinetic energy, it's important to look at the most common speeds of lithium, phosphorus (P), fluorine (F), and lithium-oxygen carbonyl (Li-OC). At 100 steps, the speed data looks good for lithium, phosphorus, and fluorine, except for how fluorine interacts with itself. So, the number of steps was increased to 2000. But even then, the particles don't spread out fully, which isn't realistic nature doesn't leave space. That's why the simulation should run up to 3000 steps for better, more realistic results.

**Keywords:** Electrolyte; Maxwell velocity distribution; Lennard Jones potential

## Introduction

To meet future electricity demands, there is a need for batteries that deliver high power while being lightweight, affordable, and safe. This growing demand has driven the development of rechargeable batteries that offer high capacity in a compact and lightweight form.<sup>1</sup> Lithium batteries are one of the most successful battery technologies over the past 20 years<sup>2</sup> Commercial lithium-ion batteries commonly use lithium hexafluorophosphate (LiPF<sub>6</sub>) dissolved in organic solvents as the electrolyte due to its high ionic conductivity. Among these solvents, ethylene carbonate (EC) is preferred because it forms a more stable solid electrolyte interphase (SEI) layer compared to other organic solvents.<sup>3,4</sup>

A commonly used anode is graphite with a lithium metal oxide cathode. Common electrolytes are lithium salts in organic solvents such as ethylene carbonate.<sup>2,5,6</sup>

Molecular simulations can provide important insights.<sup>4</sup> Molecular dynamics (MD) simulations have also been used by other researchers to study electrolyte properties.<sup>4</sup> The behavior of LiPF<sub>6</sub> in ethylene carbonate (EC) has been explored using both MD and density functional theory (DFT), focusing on how Li<sup>+</sup> and PF<sub>6</sub><sup>-</sup> interact with the solvent structure. Ab initio MD simulations have shown that Li<sup>+</sup> ions can be solvated and that their diffusion coefficient in ethyl methyl carbonate (EMC) is higher than in EC. Additionally, PF<sub>6</sub><sup>-</sup> ions diffuse faster than Li<sup>+</sup> ions. These simulations support the behavior of stable, non-degradable electrolytes.<sup>9</sup> This study aims to identify the interactions between lithium hexafluorophosphate salt and ethylene carbonate solvent during redox processes in lithium-ion batteries using classical molecular dynamics simulation.<sup>10</sup>

Jitti Kasemchainan et all focused on the interaction of LiPF<sub>6</sub> in ethylene carbonate

\*Corresponding author.

E-Mail: ngadermanh@gmail.com

(EC) solvent, examining the solvation structure involving lithium ions ( $Li^+$ ) and hexafluorophosphate ions ( $PF_6^-$ ). Their findings highlight the coordination dynamics and the role of solvent composition in affecting ion mobility. This study uses MD simulations to provide insight into how  $Li^+$  ions interact with  $PF_6^-$  in an EC environment, revealing complex interactions between solvation and ion pairing that affect ionic conductivity. They also examined how LiPF<sub>6</sub> behaves in ethylene carbonate (EC) solvents by using molecular dynamics (MD) and density functional theory (DFT), with a focus on the interactions between the solvent and the  $Li^+$  and  $PF_6^-$  ions. Siriporn Teeraburanapong et al investigated the solvation and diffusion of ions by ab initio MD simulations, showing that  $Li^+$  ions can be solvated. The diffusion coefficient of  $Li^+$  ions in EMC was shown to be larger than that in EC, and the diffusion coefficient of  $PF_6^-$  was higher than that of  $Li^+$  ions. It works on the regular and non-degradable electrolytes that the MD simulation suggests. Electrolyte degradation mechanism and its effects using molecular simulation.<sup>11</sup> The main variable in this study is velocity, which plays a central role. The system's energy is determined based on the speed of the molecules.

Because of the above background, the researcher conducted a study with the title Classical Molecular Dynamics (MD) Simulation of Salt and Solvent Solvation Events in Lithium Ion Batteries in Order to Know Energy Fluctuations and Their Effects. The simulation focuses on the interaction between  $Li^+$  and  $PF_6^-$  ions with ethylene carbonate (EC) solvent, modeled using the 12-6 Lennard-Jones potential. Solvation events, where LiPF<sub>6</sub> salt and the  $(CH_2O)_2CO$  solvent interact, are observed through the final positions of particles in the simulation results, which represent equilibrium states. These outcomes should display random symmetry across all planes. The researchers apply epsilon ( $\epsilon$ ) and sigma ( $\sigma$ ) parameters from the Lennard-Jones model, using a microcanonical ensemble system in statistical mechanics. The key independent

variable in this study is molecular velocity, from which the system's energy is derived.

This study aimed to determine the Maxwell velocity distribution. Although each molecule has different energy levels, analyzing their velocity distribution provides a clearer understanding, as velocity is directly related to kinetic energy. When lithium hexafluorophosphate (LiPF<sub>6</sub>) interacts with ethylene carbonate (EC), a solvation process occurs, resulting in random molecular motion, something observable through classical molecular dynamics (MD) simulations. The researchers used Verlet's algorithm in their coding to track particle movement, and the final positions after reaching equilibrium were recorded. The key contribution of this research is offering a new approach to MD simulation theory and coding, which could help enhance lithium-ion battery performance.

## Methods

The goal of this study was to identify the Maxwell velocity distribution. Although the approach is based on modeling through classical molecular dynamics (MD), it effectively estimates the probability distribution of molecular velocities according to Maxwell's theory. Theoretical analysis and literature review of previously published research were also conducted to provide foundational data for developing this simulation. The simulation was carried out using the Scilab software. Masia et al. later used the same parameters for unbound interactions, along with adjusted AMBER<sup>13</sup> parameters for bound interactions, to investigate the structure and vibrational characteristics of lithium ions solvated in ethylene carbonate (EC).<sup>14</sup>

The solubility of various lithium salts in ethylene carbonate (EC) and dimethyl carbonate was examined through simulations using the COMPASS force field, with ESP charges calculated using the PBE functional.<sup>15</sup> The van der Waals parameters were obtained using the automated parameter generator from Accelrys Material Studio. For unbound interactions, the parameters and



charge values for ethylene carbonate (EC) were adopted from Masia,<sup>14</sup> while the parameters for  $\text{PF}_6^-$  were sourced from Jorn,<sup>16</sup> except the Lennard-Jones sigma value for phosphorus, which was taken from the Universal Force Field (UFF).<sup>17</sup> This study applies the 12-6 Lennard-Jones potential, with all relevant parameters summarized in Table 1.<sup>18</sup> The simulation involves particles inside a box that follow Newtonian mechanics and interact using the Lennard-Jones potential. The researcher uses a system

with a constant number of particles, fixed volume, and fixed total energy (N, V, E).<sup>12</sup> The particles are contained within a box of  $l_x$ ,  $l_y$  and  $l_z$ . Initially, conditions must be set by placing the particles either evenly or randomly, ensuring they do not overlap. Each particle is then assigned an appropriate initial velocity. The motion of each particle follows the equation described in Equation 1. This equation is integrated for all particles to carry out further calculations.

**Table 1.** Non-bonded Lennard-Jones (LJ) parameters used in the simulation of  $\text{LiPF}_6$  in ethylene carbonate (EC). Here,  $O_x$  and  $C_x$  represent the carbonyl oxygen and carbon atoms, respectively;  $O_s$  refers to the ether oxygen, and C denotes the carbon atoms within the hydrocarbon structure of EC.

Atom/ Pair Types <sup>a</sup>	$\epsilon$ (Kcal/mol)	$\sigma$ (Å)
$Li$	0.10314	1.4424
$P$	0.13169	3.695
$F$	0.028716	2.9347
$Li - O_c$	0.05551	2.398

$$m \frac{d^2r_i}{dt^2} = F_i = -\nabla V \quad (1)$$

In molecular dynamics simulations, the velocity-Verlet algorithm is used to iteratively update atomic positions and velocities over time. Once the system has

reached equilibrium, we can collect and analyze statistically significant data such as temperature, pressure, and energy distributions.

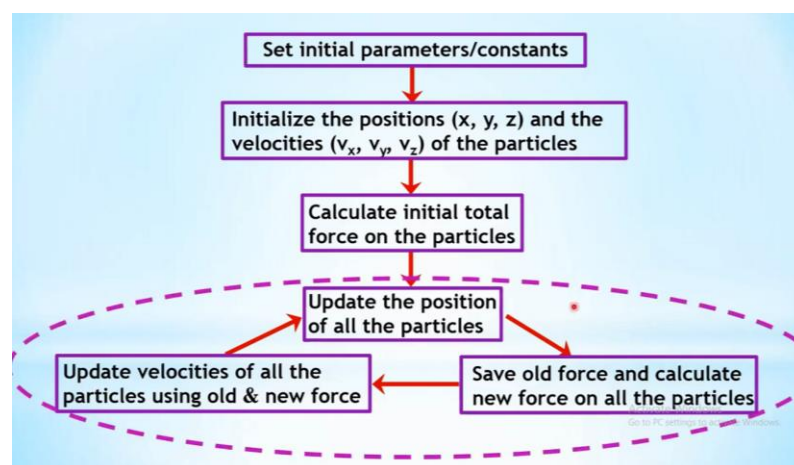


**Figure 1.** The algorithm in flowchart form, where the initial parameters or parameter constants have not been set, and then initialize the position and velocity of the particle



An overview of the algorithm is illustrated in Figure 1. The process begins with system parameters and constants yet to be defined. The positions ( $x, y, z$ ) and velocities ( $v_x, v_y, v_z$ ) All particles are then initialized. To proceed, the initial total force acting on the particles must be calculated. Using this force, the positions of all particles are updated, and the current force is stored as the "old force." Subsequently, the new force acting on the updated positions is computed. The velocities are then updated using both the old and new forces. Afterward, the positions of all particles are updated once again. These three core steps position update, force calculation, and velocity update are repeated iteratively until the system reaches equilibrium.

The potential well depth is denoted by  $\epsilon$  and  $\sigma$  represents the minimum distance at which two particles can approach each other. Figure 2 shows the initial code used to define the constants, as summarized by the researcher. In this figure, the values specific to  $\text{sig}$  and  $\text{ep}$ , which are listed in Table 1, are

```
sig=1;ep=1;m=1;lx=20;ly=lx;lz=lx;np=512;ni=2000;dt=0.005;va=3.4641016;
rc=2.5;avx=0;avy=0;avz=0;t2=0.0000125;t1=0.0025;
fc=-0.0389995;Vc=-0.0163169;
```

**Figure 2.** The initial code for defining constants is streamlined by the researcher to optimize computational efficiency and avoid unnecessary complexity.

```
// Main Program
[x,y,z]=posinit(); //position initialization
x1=x;y1=y;z1=z;
[vx,vy,vz]=velinit();
[fx,fy,fz,PEN]=forcecalc(x,y,z); //initial force calculation
for k=1:ni
[x,y,z]=updatepos(x,y,z,vx,vy,vz,fx,fy,fz); //update position
fox=fx;foy=fy;foz=fz; //save old force
[fx,fy,fz,PEN]=forcecalc(x,y,z); //update force
[vx,vy,vz,KEN]=updatevel(vx,vy,vz,fx,fy,fz,fox,foy,foz);
PE(k)=PEN/np; //average PE per particle
KE(k)=KEN/np; //average KE per particle
nit(k)=k; //no. of steps or iterations
disp('Iterations: '+string(k));
end
```

**Figure 3.** The main program includes functions for calculating the initial positions and velocities of particles and updating these values throughout the data processing phase.



simplified by assigning them a value of 1. This simplification corresponds to approximately six sets of calculation data (see Table 1). For example, one such data point corresponds to carbonyl oxygen  $O_x$ , which has values of  $\epsilon = 0.210$  and  $\sigma = 2.96$ . Figure 3 presents the main program, which includes subroutines for initializing particle positions and velocities, as well as updating them during the simulation (the subroutines themselves are not shown here). The simulation was run for 100 and 1000 iterations to ensure consistency with the Maxwell velocity distribution. The cubic simulation box has a side length ( $lx$ ) is 20, with the number of particles ( $np$ ) is 512. The box dimensions ( $ly$ ) and ( $lz$ ) are also equal to ( $lx$ ). Both kinetic and potential energy are computed, and it is essential to note that the simulation is conducted in a microcanonical ensemble ( $N, V, E$ ), where the number of particles  $N$ , volume  $V$ , and energy  $E$  are conserved. This fixed setup is used intentionally to study particle interactions within the system

The velocity of the molecules serves as the primary independent variable in most of these studies, playing a crucial role in determining which molecular species are more dominant at room temperature. From the velocity of the molecules, the energy of the system can be determined. Indeed, in the system (N, V, E), the energy is constant, but after a chemical reaction (in this case a

simulation), the speed between the molecules will experience random movements. This can be calculated based on the simulation. The code structure is shown in Figure 4, where velocity is defined as the particle's motion along the three spatial directions: x, y, and z. The histplot function is then used to provide a detailed visualization of the simulation results.

```

for i=1:np
    velocity(i)=sqrt((vx(i))^2+(vy(i))^2+(vz(i))^2);
end

//Plot Maxwell speed distribution curve
subplot(2,2,4)
histplot(20,velocity,polygon=%t);
 xlabel('Speed of the particles','fontsize',6);

```

**Figure 4.** The velocity in this code represents the particle velocity along the x, y, and z axes. The histplot function will provide a detailed description of this simulation.

In the code, Sigma  $\sigma$  is represented as "sig" and refers to the minimum distance that two particles can approach, measured in Å. The mass (m) between two molecules is represented by the reduced mass, which is set to 1 for computational simplicity during the simulation process. However, the actual reduced mass of the molecules is still taken into account when calculating the initial time. At 300 K, the energy  $kT$  of  $4,14 \cdot 10^{-21} J$ , but this value is not computed in the study to streamline the simulation process. The initial time, when the molecule is in its starting position, is provided in equation (2).

$$t = \sqrt{\frac{ml^2}{E}} \quad (2)$$

The time ( $t$ ) can be estimated by inputting the reduced mass ( $m$ ) units of  $kg$  the interatomic distance  $l$  in units of  $m$  and the molecular energy  $E$  in units of  $J$ . This results in a time scale on the order  $\sim 10^{-12} s$ .

While this paper does not include validation of the simulation results with experimental data, the epsilon ( $\epsilon$ ) and sigma ( $\sigma$ ) parameters assigned to the Lennard Jones potential formulation are obtained through experiments with a robust context. The epsilon ( $\epsilon$ ) and sigma ( $\sigma$ ) parameters are obtained through experiments and/or ab

initio DFT (where the accuracy is known). So the DFT method is used specifically to obtain the epsilon ( $\epsilon$ ) and sigma ( $\sigma$ ) parameters which are not studied in this research. The robust design has answered various realistic problems with simulation that cannot be denied because the use of DFT, MD simulation, and Monte Carlo simulation (Figure 5) has been used in various fields and has solved many problems due to trying and error done experimentally, thus reducing production costs. With the use of MD simulation and Monte Carlo, biochemists and pharmacists have found drugs that can be absorbed slowly or quickly according to consumer needs. The author does not focus too much on DFT because DFT requires a computer with sophisticated specs, like a supercomputer.

Currently, the supercomputer from the Japanese Riken company has contributed a lot to the improvement of lithium-ion battery technology by using a hybrid between DFT and MD simulation. What materials to use when there are tens of thousands of possible combinations and reactions? Scientists are looking for the best combination where new approaches have emerged for development. Yoshitaka in 2019 conducted a computer-



assisted search where computers were used to simulate the motion of individual molecules as a reference. Simulating the reaction of electrolyte molecules using this supercomputer, an unexpected thing was discovered, namely carbon dioxide was formed and the amazing thing was that when it was brought into the test, it was detected that carbon dioxide molecules were created. Likely, the molecular structure of the SEI film will also be revealed, SEI is believed to

affect the charging time. The computer will also allow researchers to understand the mechanism that leads to increased lithium conductivity. This could cut charging time to just a third of the time currently required. What is being done now is still a simulation of a small system, but it is possible in the future that large-scale simulations can be done. Computers will be able to perform more realistic and accurate simulations.

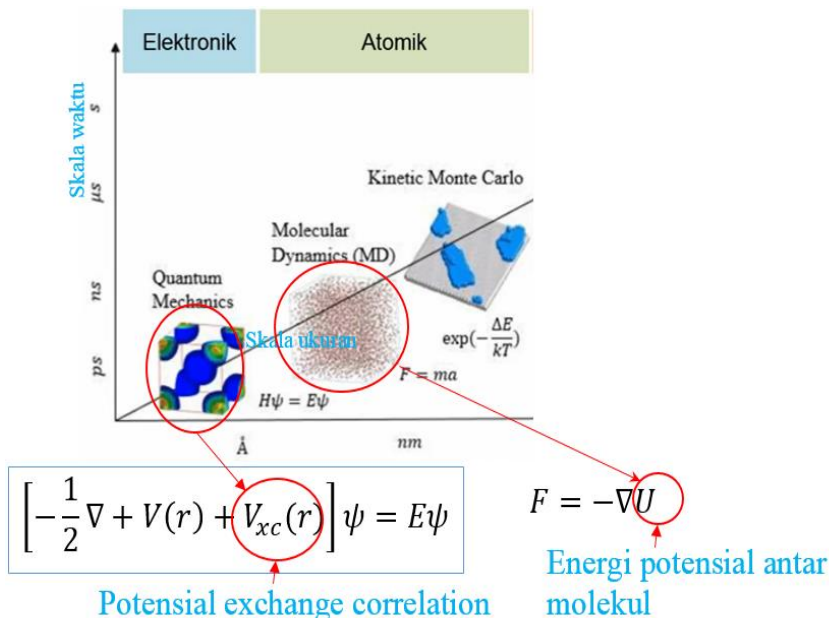


Figure 5. DFT, MD simulation, and Monte Carlo simulation

## Result and Discussion

Researchers made MD simulations using Scilab 6.11 software and obtained the results as shown in the figures below. The values for  $\epsilon$  and  $\sigma$  were obtained through MD simulations conducted using Scilab 6.11 software, and the results are presented in the figures below. The data for  $\epsilon$  and  $\sigma$  are taken from Table 1. Figures 6, 7, 8, and 9 are in the solvation event in which the  $LiPF_6$  salt interacts with the solvent ethylene carbonate  $(CH_2O)_2CO$  interact. Figure 5 for ( $Li$ ) Lithium calculation data  $\epsilon = 0.10314$  and  $\sigma = 1.4424$ , where the iteration used by researchers is 100 iterations. Figure 6 for (P) phosphorus  $\epsilon = 0.13169$  and  $\sigma = 3.695$  with 100 iterations. Figure 7 for fluorine calculation data  $F$  where  $\epsilon = 0.028716$  and  $\sigma = 2.9347$  For the case where the number of

iterations is 100, as shown in Figure 6, the peak of the Maxwell velocity distribution occurs at approximately 1.8. Figure 7 for the interaction

Between the phosphors, the iteration count is 100, the Maxwell distribution speed is 1.7. In Figures 6 to 8 the only 100 iterations, intentionally the researcher did that because specifically for visualization, the molecules will take the same part in all areas. In Figure 7, the interaction between ( $F$ ) fluorine, the curve is not regularly distributed, where there are two maximums for the Maxwell distribution velocity which is worth 1.6 and 1.85, therefore we increased the number of iterations to 2000 iterations (Figure 8). In Figure 9, the interaction between lithium and carbonyl oxygen of EC (Oc) is shown, where  $\epsilon = 0.05551$  and  $\sigma = 2.398$

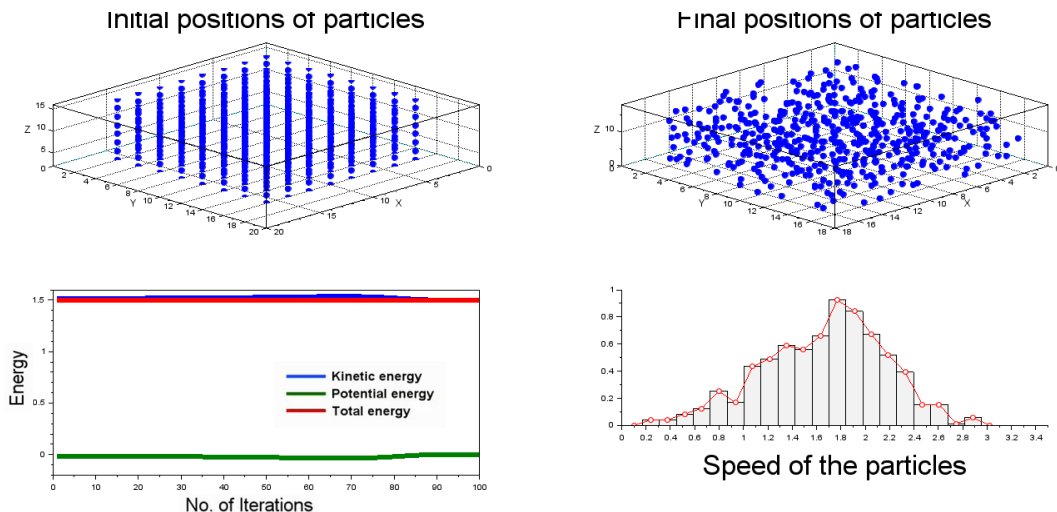


**Figure 6.** *Li* Lithium computed data  $\varepsilon = 0,10314$  and  $\sigma = 1,4424$ , The researchers used 100 iterations in their analysis.

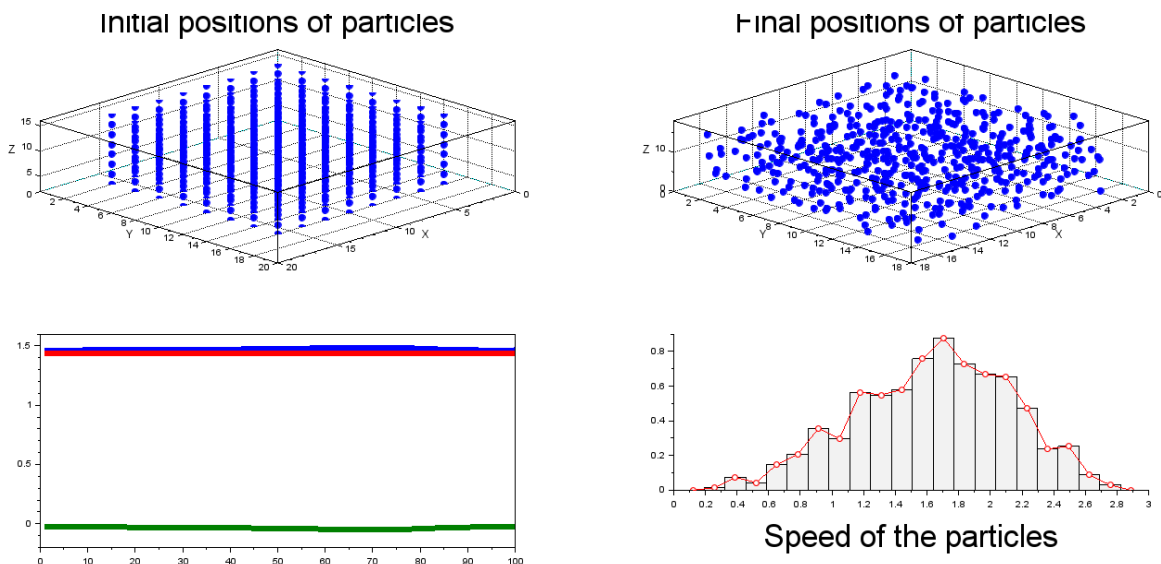


**Figure 7.** Calculation data (P) phosphorus  $\varepsilon = 0,13169$  and  $\sigma = 3,695$  The researchers employed 100 iterations in their study.

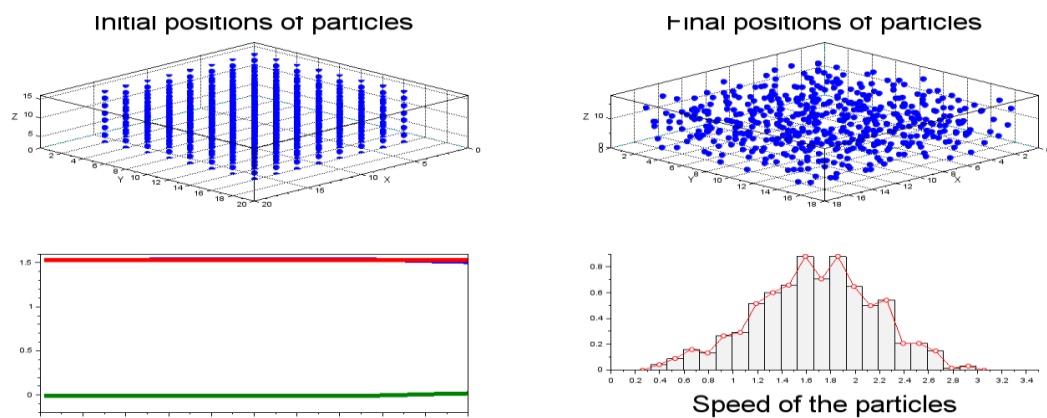


**Figure 8.** The calculated data (F) for fluorine, with  $\varepsilon = 0,028716$  and  $\sigma = 2,9347$ , was obtained using 100 iterations by the researchers.



The  $kT$  energy of 1 is inputted into the program in order to facilitate the computer in the simulation process. An energy value of  $kT$  is one input into the program to simplify the simulation process and reduce computational complexity. The initial moment, when the molecule is in its starting position, is provided in Equation (2). The corresponding time scale can be estimated by inputting the reduced mass  $m$  (kg), The distance between two atoms, denoted as  $l$ , is measured in meters (m), and the molecular energy,  $E$ , is expressed in joules (J). As a result, the time scale is typically on the order

of  $\sim 10^{-12}$  seconds. The distance between two atoms, denoted as  $l$  is set to 1 Å, which is equivalent to  $10^{-10} m$  in SI (MKS) units. The choice of  $l = 1 \text{ \AA}$  is due to the fact that the code already includes the  $\sigma$  value for each molecule. Including the exact  $\sigma$  values from the beginning would increase computational complexity. However, the researcher opted to use this approach since the number of iterations was kept below 4000. If the simulation were to run for 4000 iterations or more, it would be necessary to redefine  $\sigma = 1 \text{ \AA}$  to maintain computational efficiency.

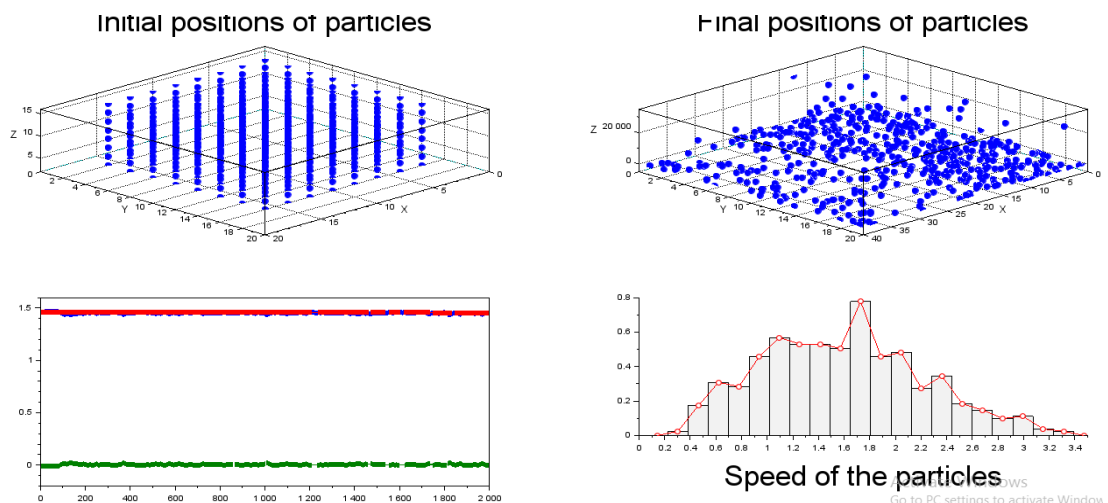


**Figure 9.** Calculation data (F) of fluorine  $\varepsilon = 0,028716$  and  $\sigma = 2,9347$ , The researchers used 2000 iterations in their analysis.

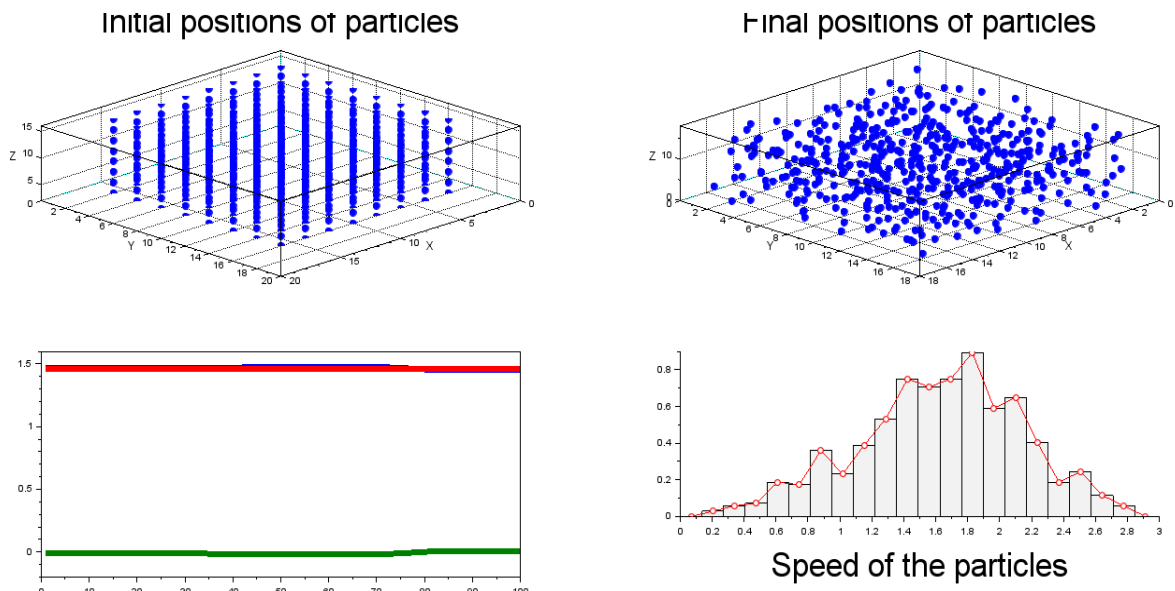


**Figure 10.** Computed results of lithium and oxygen carbonyl  $Li - OC$  where  $\varepsilon = 0.05551$  and  $\sigma = 2.398$ , The researchers used 100 iterations in their analysis.



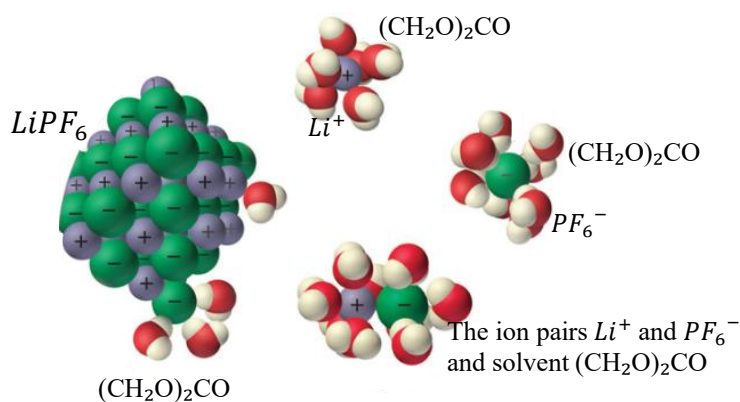


**Figure 11.** The  $Li^+$  and  $PF_6^-$  ions, when paired, migrate together as a unit. In a solution where the ions are fully dissociated, both the cations and anions are fully surrounded by solvent molecules and are free to move.

When lithium hexafluorophosphate ( $LiPF_6$ ) salt interacts with ethylene carbonate (EC) solvent, the cation  $Li^+$  binds with the anion  $PF_6^-$  and is surrounded by the EC solvent. The ion pair consists of a cation and an anion that are in direct contact within the solution, rather than separated by a solvent as can be seen in Figure 11. The ions in the ion pair are held together by the same electrostatic force found in the ionic solid. The  $Li^+$  and  $PF_6^-$  ions, as a pair, migrate together as a single unit. In the form of an ionic solid, the cation-anion interaction is constrained within a rigid structure. However, in a fully dissociated ionic solution, the cations and anions are surrounded by solvent molecules and can move freely.

In Figure 6, specifically for interaction 100, the reaction occurs during a solvation event where  $LiPF_6$  salt interacts with the solvent ethylene carbonate  $(CH_2O)_2CO$ . The molecular ion pairs  $Li^+$  and  $PF_6^-$ , along with the solvent  $(CH_2O)_2CO$ , are represented as blue spheres (for further details, refer to Figure 10). Given that the number of iterations is limited to just one hundred, the final positions of the particles exhibit random motion, nearly symmetrical across all planes (x, y, and z). This final configuration

suggests that the system has reached equilibrium.

The microcanonical ensemble described above can be linked to the canonical ensemble the (N, V, T) by treating the ensemble as a conceptual framework that records a large number of microcanonical configurations<sup>7</sup>. This logging aims to calculate thermodynamic quantities such as energy, enthalpy, Helmholtz free energy, and most importantly, Gibbs free energy, which is highly relevant to battery research. These virtual records can be linked to real-world data through probabilities, with the partition function being used within these probabilities in the ensemble. Microcanonical assemblies, canonical assemblies, and canonical ensembles are three methods used to solve problems in the microworld. While the microcanonical assemblies system may appear straightforward, the code developed by this researcher will be invaluable in determining the average energy within this system. Each molecule exhibits a range of energies, as demonstrated in the simulations shown in Figures 6, 7, 8, 9, and 10. However, these variations are more clearly observed when examining the Maxwell velocity distribution in these figures and Table 2. This microcanonical assemblies system is useful for simulating ab initio molecular dynamics. Specifically, in this study, the code used



within the microcanonical assemblies system represents an isolated system with a fixed energy. Ab initio molecular dynamics (AIMD) is an effective method for predicting the properties of molecular systems. AIMD simulations explore the potential energy surface of a system under conditions of constant energy (microcanonical) and constant temperature (canonical).

At the initial positions of the particles (as shown in Figures 6 to 10), it is assumed that no redox event has taken place, and no external force field is acting to move the molecules. External force fields may come

into play during charge and discharge events. Table 2, provides useful information in several ways, namely the most frequent speed ( $v_{mp}$ ) for lithium is  $1443 \text{ m/s}$  then the kinetic energy is  $1,77 \cdot 10^{-21} \text{ J}$ . The most frequent speed ( $v_{mp}$ ) for phosphorus P is  $1010 \text{ m/s}$  then the kinetic energy is  $8,67 \cdot 10^{-22} \text{ J}$ . The most frequent velocity ( $v_{mp}$ ) for fluorine F is  $861 \text{ m/s}$  then the kinetic energy is  $6,3 \cdot 10^{-22} \text{ J}$ . The kinetic energy is the internal energy of lithium  $Li$ , phosphorus P, fluorine F, and lithium-oxygen carbonyl  $Li - O_C$ .

**Table 2.** The initial time,  $t$ , is calculated using equation (2), along with the distance between two atoms,  $l$ , and the molecular energy,  $E$ , measured in  $\text{J}$ .

Reductio n n mass (kg)	Distance between atoms (m)	Start time $t$ (sec)	Valu e	$v_{mp}$ (m/s)	$v_{mp}$ theoretica l	$v_{avg}$ theoreti cal
Li	$5,95 \cdot 10^{-27}$	$1 \cdot 10^{-10}$	$1,2 \cdot 10^{-13}$	1,73	1443	1180
P	$1,36 \cdot 10^{-26}$	$1 \cdot 10^{-10}$	$1,81 \cdot 10^{-13}$	1,83	1010	780
F	$1,62 \cdot 10^{-26}$	$1 \cdot 10^{-10}$	$1,98 \cdot 10^{-13}$	1,7	861	716
Li	$5,91 \cdot 10^{-27}$	$1 \cdot 10^{-10}$	$1,19 \cdot 10^{-13}$	1,9	1591	1184
O <sub>C</sub>						1336

The question of whether these interactions are discrete can be answered with no, they are not. When lithium hexafluorophosphate ( $LiPF_6$ ) salt interacts with ethylene carbonate (EC) solvent, a solvation event takes place. It is well understood that in non-bonding interactions, the potential involved is the Lennard-Jones potential. The simulation of interactions between lithium ( $Li$ ), phosphorus ( $P$ ), fluorine ( $F$ ), and lithium-oxygen carbonyl ( $Li - O_C$ ) conducted in this study is based on a microcanonical assembly, representing an isolated system with constant energy ( $N, V, E$ ). The system is treated as isolated, meaning it cannot exchange energy or particles with its surroundings. While the temperature value is not included in Figures 6, 7, 8, 9, and 10, the researchers have incorporated a temperature of 300 K (room temperature) in the calculations presented in Table 2. The visualization of the molecular scattering within the ( $N, V, E$ ) system can be seen in Figures 6, 7, 8, 9, and 10. The **initial**

**positions** of the particles represent their starting state. It is important to note that this initial state is an idealized one, where the particles are symmetrically distributed throughout the entire 3-dimensional space. By using the Verlet Algorithm in the coding, the **final positions** of the particles after reaching equilibrium can be determined.

In Figure 10, for the calculated data ( $F$ ) of fluorine with  $\varepsilon = 0.028716$  and  $\sigma = 2.9347$  at 2000 iterations, the molecules in the Brownian motion pattern tend to cluster in a plane. At this stage, equilibrium has not yet been reached. We understand that there should be no empty space in this scenario, as nature tends to avoid a void. Therefore, the visualization at 2000 iterations does not accurately reflect real-world conditions. While this could occur in a brief time frame on the order of picoseconds ( $ps$ ), over time, the molecules will return to the same positions across all planes. In Figures 6, 7, 8, and 10, the iterations are limited to 100,



which is intentional for visualization purposes, as the molecules will occupy the same positions across all planes. The final goal of this research is to determine the Gibbs energy of the system, but this has not been achieved yet, as more specialized information is required. Indeed, Gibbs energy can be calculated using a microcanonical assemblies system; however, it cannot be directly applied to real-world scenarios because the system is isolated with constant energy. Systems that are more representative of the real world are canonical and grand canonical assemblies. Canonical assemblies are more commonly used because the battery (system) interacts with the environment, causing its energy to fluctuate. In this case, the system is more specifically the lithium hexafluorophosphate salt and ethylene carbonate  $(CH_2O)_2CO$  rather than the battery itself. The next goal is to develop coding for canonical assemblies simulations involving  $(N, V, T)$  and  $(N, P, T)$ . The Gibbs free energy of the reactants can be used to calculate the maximum amount of work the battery can perform. The reactants, in this case, are lithium hexafluorophosphate salt and ethylene carbonate  $(CH_2O)_2CO$ . There is a direct relationship between Gibbs free energy and cell voltage

## Conclusion

Each molecule's velocity corresponds to its kinetic energy. When lithium hexafluorophosphate interacts with ethylene carbonate, a solvation process occurs, observable through classical MD simulations. This study uses 100 and 2000 iterations to better match the Maxwell velocity distribution, within a microcanonical ensemble representing an isolated system with constant energy. Initially, no redox reactions or external forces are assumed, though such forces may arise during charging or discharging. At 2000 iterations, fluorine simulation results show molecular clustering in a plane, indicating the system hasn't reached equilibrium. Since nature tends to avoid vacuums, this visualization may not reflect real-world

behavior. Increasing the iterations to around 3000 is recommended for more accurate results.

## References

1. Septiana, Atut Reni, et al. Efek Penggunaan Cairan Ionik sebagai Aditif terhadap Konduktivitas Ionik Elektrolit Baterai Ion Litium. Indonesian Journal of Applied Physics. 2019; 9(02): 84-92.
2. Saputry, Agriccia Pangestica; Lestariningsih, Titik; Astuti, Yayuk. Pengaruh rasio LiBOB: TiO<sub>2</sub> dari lembaran polimer elektrolit sebagai pemisah terhadap kinerja elektrokimia baterai lithium-ion berbasis LTO. Jurnal Kimia Sains dan Aplikasi, 2019; 22(4): 136-142.
3. Kostecki, Robert, et al. In Situ and Ex Situ Studies of Interfacial Processes on Intermetallic Li-ion Anodes. In: Electrochemical Society Meeting Abstracts ece2019. The Electrochemical Society, Inc., 2019;(2): p. 108-108.
4. Hasa, Ivana, et al. Electrochemical reactivity and passivation of silicon thin-film electrodes in organic carbonate electrolytes. ACS applied materials & interfaces. 2020; 12(36): 40879-40890.
5. Sylvani, Miranti Maya, et al. A Review: Structure and Synthesis of Perovskite as Lithium-Ion Battery (LIB) Material. Bohr: Jurnal Cendekia Kimia. 2023; 2(01): 1-8.
6. Fu, Wenbin, et al. Materials and processing of lithium-ion battery cathodes. Nanoenergy Advances. 2023; 3(2): 138-154.
7. Gao, Tianhan; Lu, Wei. Mechanism and effect of thermal degradation on electrolyte ionic diffusivity in Li-ion batteries: A molecular dynamics study. Electrochimica Acta.2019;(323): 134791.
8. Ravikumar, Bharath; Mynam, Mahesh; Rai, Beena. Molecular dynamics investigation of electric field altered behavior of lithium ion battery electrolytes. Journal of Molecular Liquids. 2020; (300): 112252.



9. Kumar, Narendra; Seminario, Jorge M. Lithium-ion model behavior in an ethylene carbonate electrolyte using molecular dynamics. *The Journal of Physical Chemistry C*. 2016; 120(30): 16322-16332.
10. Ngaderman, Hubertus; Sinaga, Ego Srivajawaty. IDENTIFICATION OF THE INTERACTION OF LITHIUM HEXAFLUOROPHOSPHATE SALT AND ETHYLENE CARBONATE (EC) SOLVENT IN LITHIUM ION BATTERY REDOX EVENTS USING CLASSICAL MOLECULAR DYNAMICS (MD) SIMULATION. *Jurnal Neutrino: Jurnal Fisika dan Aplikasinya*. 2024; 16(2): 60-70.
11. Nogales, Paul Maldonado, et al. Effects of Electrolyte Solvent Composition on Solid Electrolyte Interphase Properties in Lithium Metal Batteries: Focusing on Ethylene Carbonate to Ethyl Methyl Carbonate Ratios. *Batteries*. 2024; 10(6): 210.
12. Mikrajuddin Abdullah. Mekanika Statistik. Bandung: Institut Teknologi Bandung; 2017
13. Gao, Tianhan; LU, Wei. Mechanism and effect of thermal degradation on electrolyte ionic diffusivity in Li-ion batteries: A molecular dynamics study. *Electrochimica Acta*. 2019; (323): 134791.
14. Behara, Pavan Kumar, et al. Benchmarking Quantum Mechanical Levels of Theory for Valence Parametrization in Force Fields. *The Journal of Physical Chemistry B*. 2024; 128(32): 7888-7902.
15. Pierini, Adriano, et al. A Polarizable Forcefields for Glyoxal Acetals as Electrolyte Components for Lithium-Ion Batteries. *ChemistryOpen*. 2024; 13(11): e202400134.
16. Choi, Sukyoung, et al. Lithium intercalated graphite with preformed passivation layer as superior anode for Lithium ion batteries. *Applied Surface Science*. 2018; (455): 367-372.
17. Naserifar, Saber; Goddard III, William A. Anomalies in supercooled water at  $\sim 230$  K arise from a 1D polymer to 2D network topological transformation. *The Journal of Physical Chemistry Letters*. 2019; 10(20): 6267-6273.
18. Hossain, Md Jamil, et al. Lithium-electrolyte solvation and reaction in the electrolyte of a lithium ion battery: A ReaxFF reactive force field study. *The Journal of chemical physics*. 2020; 152(18):

